

The simultaneous determination of air permeability and gas diffusion through ice layers in the field

G. Fortin¹, E. van Bochove², H.G. Jones³, G. Thériault² and M. Bernier³

¹Département d'Histoire et de Géographie, Université de Moncton, Moncton, Nouveau-Brunswick, E1A 3E9, Canada. E-mail: Guillaume.Fortin@umoncton.ca

²Soils and Crops Research and Development Centre, Agriculture and Agri-Food Canada, Sainte-Foy, Quebec G1V 2J3, Canada

³Institut National de la Recherche Scientifique – Eau, Terre et Environnement, Université du Québec, Québec G1K 9A9, Canada

Received 5 February 2006; accepted in revised form 1 February 2007

Abstract A coupled air permeameter–gas chamber has been used to measure both the air permeability and diffusion coefficient of an inert gas through natural ice layers. The apparatus was designed to take sequential measurements of both these parameters for the same sample without any intermediate manipulation of the specimen. In avoiding manipulation, errors related to the structural variations between different replicates are eliminated. The apparatus is portable, allowing measurements to be made directly at the study site. The permeability is directly measured *in situ* by the air permeameter while gas samples used in the diffusion experiments are collected and subsequently analysed at the laboratory. The validation of the apparatus was accomplished by comparing theoretical values for the permeability of beds of spherical beads with known dimensions. Measured permeability values, for different ice samples vary from 0.005×10^{-10} to 12.9×10^{-10} m². Mean diffusion coefficients ranged from 0.013 to 0.028 cm² s⁻¹. These values are situated in the range for those found between hard packed snow and loose compacted soil.

Keywords Gas diffusivity; ice layers; instrumentation; permeability; snow cover

Introduction

The snowpack, as a porous medium, plays an important role in the exchange between the soil and the atmosphere in high latitudes and altitudes. In temperate climates a rise of the air temperature above the freezing point or a liquid precipitation event (rain or freezing rain) are common during the winter. The results of such events can be ice layers above, within or under the snowpack. Very little data about such features in these climatic regions are available (Hardy and Albert 1993; van Bochove *et al.* 2001; Fortin *et al.* 2002) and their impacts on gaseous exchanges are poorly documented and quantified (Marsh 1991, 1999; Albert and Perron 2000). Permeability is the capability of a fluid to pass through a porous medium independently of the medium itself and it can be measured using Darcy's law. Diffusion is the displacement of a gas solely by molecular processes and it can be measured using Fick's first law (Fick 1855). Both processes are directly dependent on the structure of the porous medium (Hardy *et al.* 1995; Luciano and Albert 2002). Until now most studies have measured the two processes independently (Hardy *et al.* 1995; Winston *et al.* 1995; Albert and Shultz 2002). Different systems can be used to measure permeability, using a fluid which can either be a liquid, such as kerosene (Kuroiwa 1968), or a gas such as air (Conway and Abrahamson 1984; Hardy and Albert 1993; Sommerfeld and Rocchio 1993; Albert and Perron 2000). However, most studies used a gas chamber system to measure gas diffusivity through snow

(Winston *et al.* 1995; Jones *et al.* 1999; Sommerfeld *et al.* 1993), firm (Schwander 1996) and ice (Albert and Perron 2000). The sampler of our apparatus is used to measure both permeability and gas diffusion of ice layers, so that no snow layer measurements are taken during this experiment. Ice layers were chosen because ice plays a more significant role than does snow in gaseous and liquid exchanges between the soil and the atmosphere.

The main problem in measuring permeability and diffusivity independently is related to the local structure of the porous medium, which varies greatly for different samples even within the same ice layer (Luciano and Albert 2002). The major advantage of our apparatus is the possibility of taking measurements of the two processes (permeability and diffusivity) on the same sample without any intermediate manipulation. Hence the ice structure remains the same during the two measurements. Ice layer rotting increases with rising temperatures and most particularly when the air temperature reaches the melting point (Langham 1974). All our measurements have been made below -5°C and were taken rapidly to avoid structural change over time.

Air permeameter system design

The system was used in a series of experiments during two consecutive winters (2001–2002 and 2002–2003) to quantify air permeability and diffusivity of an inert gas through ice layers. Figure 1 shows a diagram of the apparatus. The air permeameter consists of a vacuum pump (model DOA-V191-AA, Gast Mfg. Inc. a unit of IDEX Corporation, MI) that is used to pump air through the ice sample. To control the airflow a manual valve control was used. The apparatus contains a mass flow meter (model 765, Omega Instruments Inc, IN) to measure the airflow on a scale of 0 to 200 Standard Cubic Centimeter Minutes (SCCM) with an accuracy of $\pm 1\%$ and with a repetitivity of 0.2%. A manometer (model 646-0, Dwyer Instruments Inc, IN) is used to get pressure measurements on a scale of ± 14 mm of water with an accuracy of $\pm 0.5\%$, coupled with a digital control unit (model Series16A2130, Dwyer Instruments Inc, IN) to read the values.

The sampler is an acrylic cylinder (76 mm ID, length 200 mm) with a closed end (bottom) and an open end (top). The total volume of the sampler is 455 mL (± 2 mL). Nylon tubing (0.32 mm ID) is used to join all the parts together. In the middle of the sampler a neoprene disc is fixed on an acrylic disc. A hole (10 mm ID) is located in the middle of the disc. Another similar neoprene disc is also fixed to the removable cap, in order to wedge the ice layers.

For diffusion measurements, we used the same sampler. The bottom of the sampler is closed except for two tubes that are connected to this part. Two on-off valves are fixed on

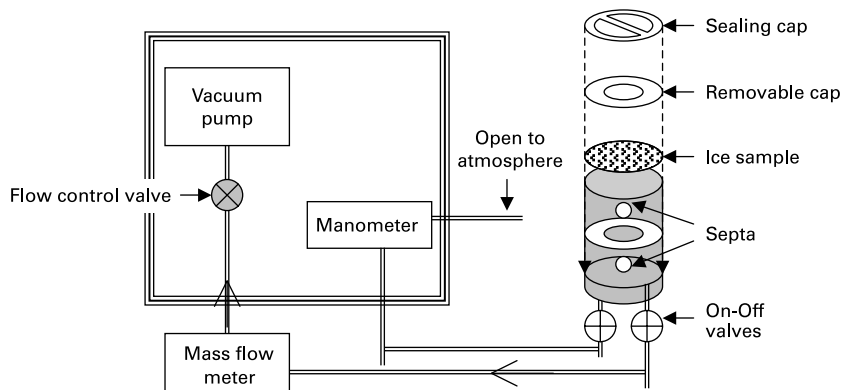


Figure 1 Schema of the air permeameter apparatus

the tubing. When those valves are closed and the sealing cap is set on the upper part, the system is then closed to the atmosphere. Finally, two septa of 22 mm ID are fixed to the wall of each chamber of the sampler to allow gas injection and sampling.

Air permeameter system performance and validation

Theoretical values. Before validating the instrument, a series of preliminary tests were conducted in the laboratory to ensure that the system was gas tight and that the gas concentration and the time between each air sample collection was appropriate. To test the tightness of the system for diffusivity measurements, we used a plastic disc instead of ice layers. Krypton (Kr) was injected in the lower chamber and we sampled the atmosphere of each chamber after regular time intervals of 5 min for the first hour and then let it stand for 48 h. No significant leaks were observed, meaning that less than 5% of the initial volume of Kr was transferred from the lower chamber to the upper chamber after 48 h.

Subsequently, the permeameter was validated in the laboratory by comparing theoretical values with measured values. This was done using spherical glass beads of known diameter of different ranges: 0.25–0.177; 0.15–0.105; 0.09–0.063 mm. The diameter ranges of those particles are equivalent to those of natural ice grains or snow crystals.

To calculate theoretical permeability values, two empirical methods were chosen: the Rumpf and Gupte (1971) phenomenological model and the Carman–Kozeny approach (Carman 1937, 1938, 1956; Kozeny 1927). These methods use only a mean glass bead diameter and a porosity function based on an experimental dataset. The Rumpf and Gupte phenomenological model shows that a non-dimensional relationship exists between the following parameters:

$$\frac{\Delta P}{\rho v^2} = f\left(\frac{v\bar{D}_p}{vz/\bar{D}_p}, \phi, q_i, \psi_i, \text{structure}\right) \quad (1)$$

where ΔP = pressure gradient for distance z (bed thickness), ρ = density, v = filter velocity, v = velocity, \bar{D}_p = mean particle diameter, ϕ = bulk porosity, q_i = distribution parameters for the particles size, ψ_i = parameters for the particle shape, structure = particles' compactness.

To obtain the permeability value using the previous model, we use the Darcy law in the following way:

$$k = \frac{\bar{D}_{p2}^2 \phi^{5.5}}{5.6K} \quad (2)$$

where \bar{D}_{p2}^2 = areal mean particle diameter, K = constant (value 1.00).

In the literature, porosity functions are used with exponents that vary from 1 to 6. Following Dullien (1992) the use of spherical particles justified the use of the function $f(\phi^{5.5})$. The choice of this function can greatly affect the theoretical values of permeability. All of the structural parameters of the particles, such as porosity and tortuosity, vary and are difficult to evaluate, which partially explains the large variation of the calculated porosity function.

The Carman–Kozeny model gave relatively similar results, as shown in Figure 2. Assuming that the particles are spherical, the following equation is used to get the Carman–Kozeny permeability:

$$k_{CK} = \left(\frac{\bar{D}_{p2}^2}{180}\right) \left[\frac{\phi^3}{(1-\phi)^2}\right]. \quad (3)$$

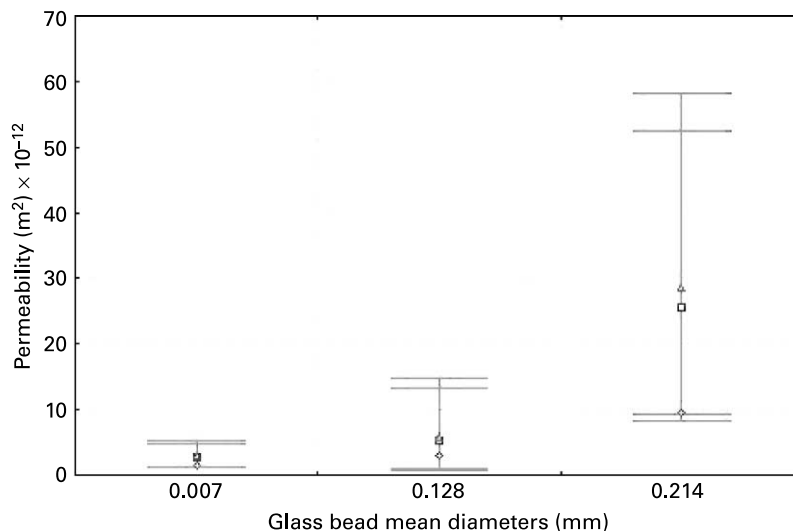


Figure 2 Theoretical permeability values [Carman–Kozeny (Δ); Rumpf and Rupte (\square)] versus measured values (\diamond) for different glass bead diameter ranges

Using a range of glass bead diameters instead of a uniform glass bead pack could affect the precision of the theoretical values obtained, but no other testing medium was available at the time of experimentation. We calculated variations of theoretical permeability of more than 200% within the same glass bead diameter range. This high fluctuation indicated that even a small change in the spherical diameter can greatly affect the permeability value. For each size of glass bead, Figure 2 presents the observed mean, the maximum and minimum permeability values, and compares them to values calculated using both the Rumpf and Gupte and the Carman–Kozeny models.

When using the Carman–Kozeny model, it was particularly important to use an accurate porosity value since, as for the Rumpf and Gupte model, a simple change in the porosity value could greatly affect the permeability value. Figure 2 shows the comparison between the theoretical values from the two models and the measured values from the permeameter. This figure clearly shows that the three datasets follow the same tendency even if the measured data are slightly below two calculated values. After a series of investigations, in which glass bead diameters were measured under the microscope and porosity was calculated by immersion methods (Dullien 1992), it was concluded that the systematic bias in permeability measurements was caused by the apparatus. Knowing that the relationship between the airflow and the pressure gradient is linear, a simple modification of one of the parameters was directly translated by a modification of the other parameter. Still, the values measured are in the same range as the theoretical values, which indicates that the air permeameter apparatus is stable and reliable.

Sampling methods

The field data was collected at the J.-C. Chapais Experimental Farm of Agriculture and Agri-Food Canada (46°46'18"N, 71°12'15"W near Quebec City, Quebec, Canada). After digging a snowpit and measuring standard snowpack properties (Fortin 2003), some ice samples for each ice layer were gently removed from the snow cover and cut with a saw to fit into the ice sampler. The snow surrounding each ice layer sample was gently removed with a paintbrush to keep only the thin ice layer. The samples were then carried to a sheltered area, isolated from airflow that can be created by wind, where the air permeability and diffusivity

measurements were taken. A particularly careful manipulation was done to avoid destroying the fragile structure of the thin ice layers. Before mounting the ice sample in the sampler, a light collar of petroleum jelly (kept at a temperature below 0°C) was added above and below each neoprene disk to minimize the risk of leaks between the ice sample surface and the neoprene. The ice sample was gently placed in the sampler and the removable cap was put in place.

Permeability measurements were taken first. The air permeameter was used to measure the volumetric airflow, Q ($\text{m}^3 \text{s}^{-1}$), with the mass flow meter, and the pressure gradient, ΔP (Pa), with the manometer, between the inner chamber and the atmosphere. With these two parameters we have calculated the air permeability (k) of ice layers using Darcy's law as:

$$k = \frac{Q}{A} \left(\frac{\Delta P}{L \mu_f} \right) \quad (4)$$

where Q = the volumetric flow ($\text{m}^3 \text{s}^{-1}$), A = the surface area (m^2), ΔP = the pressure gradient (Pa), L = the distance (m) of ΔP , μ_f = the dynamic viscosity of air ($\text{kg m}^{-1} \text{s}^{-1}$) in known conditions.

A valve was used to control the airflow rate, starting with no flow and then gradually increasing it. The pressure gradient changes between the inner chamber and the atmosphere were noted. To ensure more accurate data, four measurements were taken for each ice sample. Once the permeability measurements were finished, the same sample was used for diffusion measurements.

With the sample left in place, the sealing cap was added to the top of the upper chamber and the two on-off valves were closed on the tubing, thus obtaining a closed system constituted by two chambers separated by the ice sample. To calculate D_s we used the Stokes's cell method (Stokes 1950) as:

$$D = \frac{1}{\beta t} \ln \left[\frac{(c_{1,\text{bottom}} - c_{1,\text{top}})_{\text{initial}}}{(c_{1,\text{bottom}} - c_{1,\text{top}})_{\text{at.time } t}} \right] \quad (5)$$

where β = diaphragm-cell constant (cm^2), t = time (s), c_1 = solution concentrations under various conditions.

The diaphragm-cell constant, β , is obtained by

$$\beta = \frac{A}{l} \left(\frac{1}{V_{\text{top}}} + \frac{1}{V_{\text{bottom}}} \right) \quad (6)$$

where A = available area for diffusion (cm), l = effective thickness of diaphragm (cm), V_{top} and V_{bottom} = cell compartment volume (mL).

Each chamber had its own septum on the cylinder wall to insert and collect gas samples. For the diffusivity measurement, a Kr gas cylinder was required at the field site. A manometer equipped with a septum was fixed to the Kr gas cylinder to permit gas sampling. Using a syringe, a volume of 45 mL of pure Kr (which represents 10% of the total volume of the chamber) was injected into the lower chamber via the septum. The initial concentration of the upper chamber was at atmospheric concentration. Every minute after the initial injection in the lower chamber an air atmosphere sample of each chamber was collected and injected into a 7 mL vial. Afterwards the vials were brought to the laboratory for analysis.

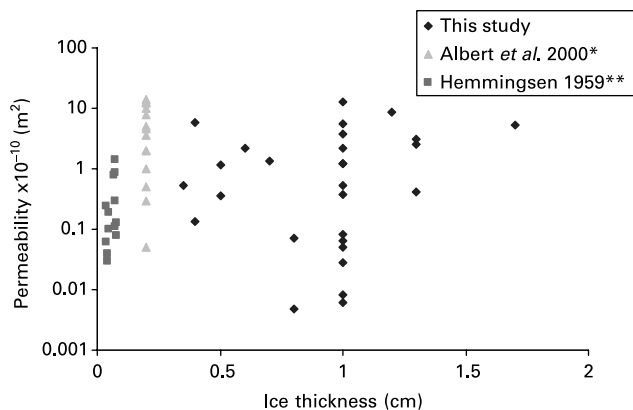
The Kr was analyzed by gas chromatography (Agilent Technologies GC 6890N) equipped with a TCD detector. The operating set-up and conditions were as follow: a Porapak Q column (100/120 mesh), 1.859 m long by 0.32 cm ID, He as carrier gas (25 mL min^{-1}), oven temperature at 50°C, injection port temperature at 110°C, detector temperature at 150°C. The injection volume was 50 μL .

Because diffusion and permeability measurements were quite sensible to the wind effect, which can create pressure differentials, ice samples were collected and measurements were taken *in situ* in a non-heated shed in the field, where the air temperature was constant and the wind impact on measurements was minimized. All the measurements were made at a temperature within the manufacturer's suggested limits for the instruments, which was above -10°C .

Results

The permeability and diffusivity results were in close agreement with other data found in the literature. However, very little data on the air permeability of natural ice layers was found. Our values, 0.05×10^{-10} to $12.9 \times 10^{-10} \text{ m}^2$ (Figure 3), are in the same range as those measured by Albert and Perron (2000), 0.05×10^{-10} to $19 \times 10^{-10} \text{ m}^2$. Hemmingsen (1959) had created artificial ice layers in a cold laboratory and observed permeability that varied from 0.03 to $1.14 \times 10^{-10} \text{ m}^2$ as shown in Figure 3. These artificial ice layers are relatively similar to those found in this study. As mentioned previously during the validation of the apparatus a large variation was observed in permeability values. A simple reorganization of the same beads in a different pack structure resulted in up to 200% variation in permeability values. It shows the importance of structural parameters, such as porosity and tortuosity, on permeability. The heterogeneous structure of a natural ice layer is obviously more complex than a perfectly spherical glass bead pack, which explains the large order of magnitude within the permeability measurements. Snow distribution on the ground can also modify the ice layer's properties but the structural parameters seem to be the leading factor, since they change over very short distances as well as over time in accordance with Langham's (1974) field observations.

The diffusivity values obtained by experimentation varied from 0.006 to $0.41 \text{ cm}^2 \text{ s}^{-1}$ (Figure 4). They varied between values obtained for a dense and compacted snowpack, 0.02 to $0.5 \text{ cm}^2 \text{ s}^{-1}$ for CO_2 (Winston *et al.* 1995) and a coarse sandy loam, 0.0077 to $0.0174 \text{ cm}^2 \text{ s}^{-1}$ (van Bochove *et al.* 1998). Permeability and diffusivity were closely related to structural parameters of snow and ice (Fortin 2003). More investigation is required clearly to established a quantitative relationship between permeability and diffusion processes even though they seem to be driven by the structural parameters of the ice layers, such as tortuosity, that restrict the way gases can pass through the ice.



* = Ice thickness value is not specified for each permeability value so a mean value have been given

** = Those values are for artificial ice layers instead of natural ice layers

Figure 3 Comparison of ice layers permeability from different sources including those collected with the apparatus

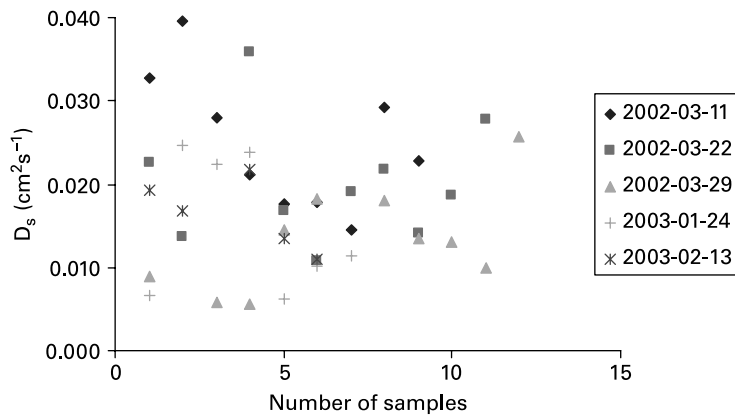


Figure 4 Various diffusion coefficients (D_s) obtained at different times using the apparatus

Conclusion and remarks

The permeability and diffusivity measurements were in accordance with those found in the literature. The functionality of the air permeameter apparatus and the possibility of using only one apparatus for both permeability and diffusivity represented a significant advantage. For example, the results can be compared to see the relationship between both processes on the same ice sample. This portable apparatus has a temperature range of operation, but that limitation can be surpassed by using another mass flow meter model. It is also necessary to use the apparatus in a closed area to avoid wind disturbance. A data logger could be used to replace the digital unit to save time and to produce a more detailed database. The equivalent permeability and diffusivity must be taken to give an overview of the entire snowpack restriction effect for gaseous and liquid exchanges between soil and atmosphere components. More investigation is required in the future to detail and quantify the relationship that exists between the natural ice layer's structural properties and its impact on gaseous and liquid exchanges between soil and atmosphere components.

Acknowledgements

We thank the Agriculture and Agri-Food Canada staff for excellent field support at the experimental farm study site. This work was made possible by financial support from the CRYSYS program (Environment Canada).

References

- Albert, M.R. and Perron, F.E. (2000). Ice layer and surface crust permeability in a seasonal snow pack. *Hydrol. Process.*, **14**, 3207–3214.
- Albert, M.R. and Shultz, E.F. (2002). Snow and firn properties and air-snow transport processes at Summit. *Greenland. Atmos. Environ.*, **36**, 2789–2797.
- Carman, P.C. (1937). Fluid flow through a granular bed. *Trans. Inst. Chem. Engrs.*, **15**, 150–167.
- Carman, P.C. (1938). Fundamental principles of industrial filtration. *Trans. Inst. Chem. Engrs.*, **16**, 168–183.
- Carman, P.C. (1956). *Flow of Gases Through Porous Media*, Butterworths, London.
- Conway, H. and Abrahamson, J. (1984). Air permeability as a textural indicator of snow. *J. Glaciol.*, **30**(106), 328–333.
- Dullien, F.A.L. (1992). *Porous Media; Fluid Transport and Pore Structure* (2nd edn), Academic Press, San Diego.
- Fick, A. (1855). Über Diffusion. *Ann. Phys.*, **94**, 59.
- Fortin, G. (2003). *Conceptualisation des processus de formation, d'évolution et de désagrégation des couches de glace dans un couvert nival saisonnier*. PhD thesis, Institut National de la Recherche Scientifique (INRS-EAU), Université du Québec.

- Fortin, G., Jones, H.G., Bernier, M. and Schneebeli, M. (2002). Changes in the structure and permeability of artificial ice layers containing fluorescent tracer in cold and wet snow cover. In: *59th Eastern Snow Conference Proceedings, Stowe*, 5–7 June. pp. 257–266. Available at: <http://www.easternsnow.org/proceedings.html>
- Hardy, J.P. and Albert, D.G. (1993). The permeability of temperature snow; preliminary links to microstructure. In: *Eastern Snow Conference Proceedings, Québec*, 8–10 June. pp. 149–156.
- Hardy, J.P., Davis, R.E. and Winston, G.C. (1995). Evolution of factors affecting gas transmissivity of snow in the boreal forest. In: Tonnessen, K., Williams, W.K., Tranter, M. (Eds.). *Biogeochemistry of Seasonally Snow-Covered Catchments. Proceedings of a Boulder Symposium, July*. IAHS Vol. 228, pp. 51–59.
- Hemmingsen, E. (1959). Permeation of gases through ice. *Tellus XI*, **3**, 355–359.
- Jones, H.G., Pomeroy, J.W., Davies, T.D., Tranter, M. and Marsh, P. (1999). CO₂ in Arctic snow covers: landscape form, in-pack gas concentration gradients, and the implications for the estimation of gaseous fluxes. In: *56th Eastern Snow Conference Proceedings, Fredericton*, 2–4 June. pp. 233–245.
- Kozeny, J.S. (1927). *Über Kapillare Leitung des Wassers im Boden*. Sitzungsberichte der Akademie der Wissenschaften in Wien. Abteilung IIa.
- Kuroiwa, D. (1968). Liquid permeability of snow. In: *General Assembly of Bern, 25 September–7 October 1967*. Commission of Snow and Ice, Reports and Discussion. IAHS, Vol. 79, pp. 380–391.
- Langham, E.J. (1974). *The Mechanism of Rotting Ice Layers within a Structured Snowpack*. IAHS, 114. pp. 73–81.
- Luciano, G.L. and Albert, M.R. (2002). Bidirectional permeability measurements of polar firn. *Annals Glaciol.*, **35**, 63–66.
- Marsh, P. (1991). Water flux in melting snow covers. In M.Y. Corapcioglu (Ed.), *Advances in Porous Media I*, Elsevier, New York. pp. 61–122.
- Marsh, P. (1999). Snowcover formation and melt: recent advances and future prospects. *Hydrol. Process.*, **13**, 2117–2134.
- Rumpf, H. and Gupte, A.R. (1971). Einflüsse der Porosität und Korngrößenverteilung im Widerstandsgesetz der Proenstromung. *Chemie Ingenieur Technik.*, **43**, 367–375.
- Schwander, J. (1996). Gas diffusion in firn. In E.W. Wolff and R.C. Bales (Eds.), *NATO ASI Series I: Chemical Exchange Between the Atmosphere and Polar Snow* (Vol. 143), Springer-Verlag, Berlin. pp. 527–540.
- Sommerfeld, R.A., Mosier, A.R. and Musselman, R.C. (1993). CO₂, CH₄ and N₂O flux through a Wyoming snowpack and implications for global budgets. *Nature*, **361**, 140–142.
- Sommerfeld, R.A. and Rocchio, J.E. (1993). Permeability measurements on new and equitemperature snow. *Water Res. Res.*, **29**(8), 2485–2490.
- Stokes, R.H. (1950). The Diffusion Coefficients of eight Uni-univalent Electrolytes in Aqueous Solution at 25°. *J. Am. Chem. Soc.*, **72**, 2243–2247.
- van Bochove, E., Bertrand, N. and Caron, J. (1998). In situ estimation of the gaseous nitrous oxide diffusion coefficient in a sandy loam soil. *Soil Sci. Soc. Am. J.*, **62**, 1178–1184.
- van Bochove, E., Thériault, G., Rochette, P., Jones, H.G. and Pomeroy, J.W. (2001). Thick ice layers in snow and frozen soil affecting gas emissions from agricultural soils during winter. *J. Geophys. Res. – Atmos.*, **106**(D19), 23061–23072.
- Winston, G.C., Stephens, B.B., Sundquist, E.T., Hardy, J.P. and Davis, R.E. (1995). Seasonal variability in CO₂. In: Tonnessen, K., Williams, W.K., Tranter, M. (Eds.). *Biogeochemistry of Seasonally Snow-Covered Catchments*. IAHS, Vol. 228, pp. 61–70.